Model Based Estimation of Fractional Dimension with Applications to Image Texture Analysis

Szu–Chu Liu and Shyang Chang

Dept. of Electrical Engineering, National Tsing Hua University
Hsinchu, Taiwan, Republic of China

Abstract

Recently, the *fractional Brownian motion* (FBM) with parameter H has been used as a description model for a large number of natural shapes and phenomena. In practice, it is essential to estimate the parameter H, or the fractal dimension defined by D=2–H, from a given data set. In this paper, we will propose a new method to estimate fractal dimension by applying the autoregressive (AR) model-based approach to estimate the power spectral density of *discrete-time fractional Gaussian noise* (DFGN), which is the increment of discrete-time FBM (DFBM). In the simulation results, we will see that the variance be smaller than those obtained by previous methods. Finally, several natural textured images are analyzed by making use of the proposed estimation method.

I. Introduction

Many objects and shapes in the natural world possess the property of '*scale-invariance*' or '*self-similarity*', which means that portions of the patterns will be similar to the original one with increasing magnification. A model used to describe such characteristic is *fractal* [1] which receives increasing attention in many fields. An interesting fact is that most of the natural scene images can be assumed fractals over a wide range of scales. For example, if the length of a coastline is measured using different sizes of rulers, Mandelbrot [1] has shown that the relationship between the ruler size ϵ and the measured length $L(\epsilon)$ will be

$$L(\epsilon)=F\epsilon^{1-D} \qquad (1)$$

where F is the proportional constant and D the *fractal dimension*. Fractal dimension will be a consistent description of the roughness of a curve in the manner that the curve is a smooth line for D=1 and becomes more rugged as D increases to 2. In practice, natural patterns and phenomena are only *statistically* scale invariant and should be modeled as random functions. It has been proposed by Mandelbrot [2] since 1968 that *fractional Brownian motion* (FBM) can be used as a description model for a vast number of such phenomena and objects. The definition of FBM with exponent H involving stochastic integral was given in [2]. Let $(\Omega,\mathcal{A},\mathbb{P})$ be the underlying probability space and $B_H(t,\omega)$ denote FBM with exponent H. The variance of $[B_H(t+T,\omega) - B_H(t,\omega)]$ can be evaluated by

$$E\left\{\left[B_H(t+T,\omega) - B_H(t,\omega)\right]^2\right\} = T^{2H} V_H \qquad (2)$$

where V_H is a constant. Alternatively, we can write

$$\mathbb{P}(\{\omega: \frac{B_H(t+T,\omega)-B_H(t,\omega)}{|T|^H} < y\}) = F(y) \qquad (3)$$

where F(y) is the cumulative distribution function of Gaussian distribution with mean zero and variance V_H. Since FBM is Gaussian, it follows from above that the increments of $B_H(t,\omega)$ are *self-similar*, i.e.,the two random functions $\{B_H(t_0+\tau,\omega) - B_H(t,\omega)\}$ and $\{h^{-H}[B_H(t_0+h\tau,\omega) - B_H(t_0,\omega)]\}$ have the same distributions. In fact, the behavior of FBM depends only on the parameter H, to which the fractal dimension for a one-dimensional FBM can be expressed as

$$D=2–H. \qquad (4)$$

It is also worthy of noting that FBM is almost surely not differentiable and hence the definition of the 'derivative' of FBM is meaningless. However, we may define the derivative of FBM, which is called *fractional Gaussian noise* (FGN), as being a generalized random function in the sense of Schwartz distributions [2]. Mandelbrot also showed that FGN is stationary and has a power spectral density (PSD) proportional to $|f|^{1-2H}$, where f denotes frequency. Thus, the graph will be a straight line with slope S=1–2H if we plot the PSD of FGN, $P_H(f)$, versus f in log-log scale for $0 \le f \le 0.5$. We

can obtain the expression for the fractal dimension of FBM as (3+S)/2.

The discrete-time FBM (DFBM) can be obtained by sampling FBM at an equally spaced period T_S, i.e.

$$B_H[n,\omega]=B_H(nT_S,\omega) \tag{5}$$

where the bracket and parentheses denote the discrete-time and continuous-time data, respectively. We now define DFGN as the increment of DFBM, which can be written as

$$X_H[n,\omega]=B_H[n,\omega]-B_H[n-1,\omega]. \tag{6}$$

To simplify the notation in the following, we will use $B_H[n]$ and $X_H[n]$ to denote DFBM and DFGN, respectively. Mandelbrot showed that $X_H[n]$ is a discrete strict sense stationary Gaussian process with mean zero and autocorrelation $r_H[k]$ which can be evaluated by

$$r_H[k] = \frac{\sigma^2}{2}\left[|k+1|^2 -2|k|^2 +|k-1|^2\right] \tag{7}$$

where σ^2 is the variance of $X_H[n]$.

In practice, it is imperative to estimate the fractal dimension from a given data set in the applications of FBM model and several methods are proposed by other authors in the past (see [3] and [4]). In this paper, we propose a new method to estimate the fractal dimension from data by AR model-based spectral estimation. The results from other authors will be compared with ours in Section IV.

II. The Spectra of DFGN

A critical problem of aliasing will occur when we sample FGN to DFGN since the PSD of FGN is not bandlimited. This implies that the PSD of DFGN may not be exactly proportional to $|f|^{1-2H}$ as in the continuous-time case. A straightforward method to evaluate the PSD of DFGN is to take Fourier transform on the autocorrelation function of DFGN. By doing this, we will get

$$P_H(f)= r_H[0] + 2\sum_{k=1}^{\infty} r_H[k]\cos(2\pi fk) \tag{8}$$

where $r_H[k]$ is given in (7).

There are several problems in the analytic evaluation of (8). Because of these analytic difficulties, we now proceed to evaluate the PSD of $x_H[n]$ numerically. First, the frequency interval [0,0.5] is equally spaced into 64 points. To avoid the singularity of the PSD of DFGN, let $F_M=\{f_1,..., f_M\}$ be the frequency partition of (0,0.5) satisfying the inequalities

$$0 = f_0 < f_1 < ... < f_M < f_{M+1} = 0.5 \tag{9}$$

where $f_i - f_{i-1} = 0.5 / (M + 1)$ for i = 1, 2,..., (M + 1) with M=62. Thus, the values of the PSD of DFGN at F_M, which is denoted by $P_H(F_M)= \{P_H(f_i)\}$ for i = 1, ..., M, can be obtained by computing (8) numerically. In the numerical procedure, the autocorrelation function $r_H[k]$ is computed and summed until k = 60,000 or $|r_H[k]| < 0.00001$. If we illustrate $P_H(F_M)$ versus F_M in the log-log scale for various H, these plots are nearly straight lines and can be described by the linear equation

$$\log(P_H(f)) = S(H)\cdot\log(f) + T(H). \tag{10}$$

Thus S(H) can be obtained by linear regression as

$$S(H) = \frac{\sum_{i=1}^{M} y_i x_i - M\bar{y}\bar{x}}{\sum_{i=1}^{M} x_i^2 - M\bar{x}^2} = \sum_{i=1}^{M} \alpha_i y_i \tag{11}$$

where $x_i = \log(f_i)$, $y_i = \log(P_H(f_i))$, $\bar{x} = \frac{1}{M}\sum_{i=1}^{M} x_i$, $\bar{y} = \frac{1}{M}\sum_{i=1}^{M} y_i$, and

$$\alpha_i = \frac{x_i - \bar{x}}{\sum_{i=1}^{M} x_i^2 - M\bar{x}^2}. \tag{12}$$

Note that S(H) derived by this way does not correspond to (1–2H), even though it is true for FGN. However, the function h which maps S(H) into (0,1) should be one–to–one and continuous. The computed S(H)'s versus the H's which range from 0.05 to 0.9 with increments 0.025 are plotted in Fig. 1. Hence, we can represent h by a quadratic function having the least squared error defined by

$$\sum_{k=1}^{35} [\, H(k)-h(S(k))\,]^2$$

where H(k) and S(k) are defined by H(1)=0.05 and H(k+1)–H(k)=0.025 and S(k) is the corresponding slope computed for H(k) for k=1, ..., 35. We then obtain

$$h(x)=h_0+h_1x+h_2x^2 \tag{13}$$

with

$$h_0=0.4959,\ h_1=-0.4224,\ \text{and}\ h_2=0.0622. \tag{14}$$

The relationship between S(H) and H, and the function h are depicted in Fig. 1, where we can see that the function h fits the points (S(H),H) very well for H=0.05, ..., 0.9. Moreover, the inverse function of h will exist in the S(H) domain and can be represented by

$$g(y)=g_0-\sqrt{g_1+g_2y} \tag{15}$$

with

$$g_0=-\frac{h_1}{2h_2},\ g_1=\left[\frac{h_1}{2h_2}\right]^2-\frac{h_0}{h_2},\ \text{and}\ g_2=\frac{1}{h_2}. \tag{16}$$

From this we note that DFGN has a PSD proportional to $f^{g(H)}$ instead of $f^{(1-2H)}$ as inferred previously.

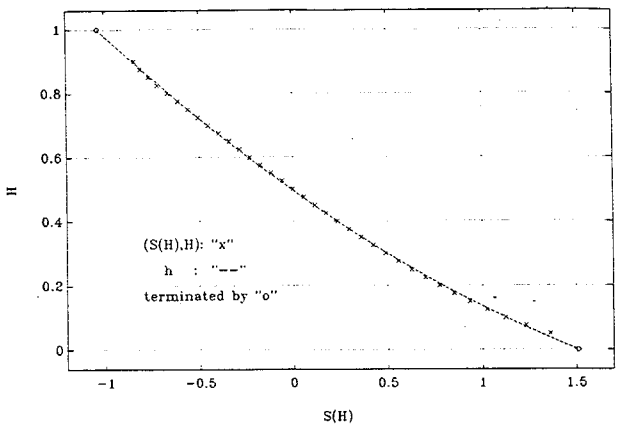

Fig. 1. Graphs of (S(H),H) and function h.

III. Model–Based Estimation of Fractal dimension

The algorithm to estimate parameter H (and hence fractal dimension D) of DFBM or DFGN will be developed in this section. According to Wold's and Kolmogorov's theorems (see [5]), we can approximate the DFGN data, {x[n],n = 1, 2,..., N}, by an AR(p) model with an appropriate order p as follows:

$$x[n]=-\sum_{k=1}^{p} a_p[k]x[n-k]+u[n], \text{ for } n=p+1, \ldots, N \qquad (17)$$

where $a_p[k]$'s are the coefficients of AR model and u[n] a white Gaussian noise with mean zero and variance σ_u^2. The estimates of $\mathbf{a}$, $\hat{\mathbf{a}} = [\,-\hat{a}_p[1] \;\; -\hat{a}_p[2] \cdots -\hat{a}_p[p]\,]'$, will be determined by minimizing the following cost function

$$V(\mathbf{a}) = \frac{1}{2}\sum_{n=p+1}^{N} (u[n])^2 = \frac{1}{2}\,\mathbf{u}'\mathbf{u} \qquad (18)$$

where $\mathbf{u}=[\,u[p+1]\; u[p+2] \cdots u[N]\,]'$. Suppose that the matrix $\Phi'\Phi$ is positive definite, then $V(\mathbf{a})$ has a unique minimum at

$$\hat{\mathbf{a}} = (\Phi'\Phi)^{-1}\Phi'\mathbf{x} \qquad (19)$$

and the estimate of the variance of u[n], denoted by $\hat{\sigma}_u^2$, is the corresponding minimal value of $V(\mathbf{a})$, or,

$$\hat{\sigma}_u^2 = V(\hat{\mathbf{a}}) = \frac{1}{2}\left[\mathbf{x}'\mathbf{x} - \mathbf{x}'\Phi(\Phi'\Phi)^{-1}\Phi'\mathbf{x}\right] \qquad (20)$$

where $\mathbf{x}=[\,x[p+1]\; x[p+2] \cdots x[N]\,]'$ and

$$\Phi = \begin{bmatrix} x[p] & \cdots & x[1] \\ x[p+1] & \cdots & x[2] \\ \vdots & \ddots & \vdots \\ x[N-1] & \cdots & x[N-p] \end{bmatrix}. \qquad (21)$$

Next, we make use of Akaike's information criterion (AIC) [6] to determine the model order $\hat{p}$. Specifically, the best choice of the model order will be

$$\hat{p} = \text{argument}\{\min_{p} [N\cdot\log(\hat{\sigma}_u^2) + 2p]\}. \qquad (22)$$

As soon as $\hat{\mathbf{a}}$, $\hat{\sigma}_u^2$ and $\hat{p}$ are determined by (19), (20) and (22), the estimate of the fitted AR PSD can be obtained by substituting $\hat{\mathbf{a}}$ and $\hat{\sigma}_u^2$ into the theoretical PSD expression for AR model, i.e.,

$$\hat{P}(f)=\frac{\hat{\sigma}_u^2}{|1+\hat{a}[1]\exp(-j2\pi f)+ \cdots +\hat{a}[\hat{p}]\exp(-j2\pi f\hat{p})|^2}. \qquad (23)$$

We now evaluate the slope of the log-log plot of $\hat{P}(F_M)$ versus F_M by linear regression as

$$\hat{S} = \sum_{i=1}^{M} \alpha_i \cdot \log(\hat{P}(f_i)), \qquad (24)$$

and define the estimate for the parameter H of DFGN as

$$\hat{H} = h(\hat{S}) \qquad (25)$$

where the constants α_i's and function h are defined as in (12)-(14). Finally, estimate of the fractal dimension of {x[1], ⋯, x[N]} is

$$\hat{D} = 2 - \hat{H}. \qquad (26)$$

IV. Simulation Results

Since the bias and variance of the proposed estimator cannot be derived analytically, we will show its performance by simulations in this section. The DFGN data is generated by the procedure proposed in [4]. After the DFGN data are generated, we proceed to estimate the PSD by fitting them to an AR(p) model. To estimate the coefficients of AR model, we make use of the ARX subroutine supported in MATLAB. Furthermore, the optimum order which minimizes AIC for AR model will be chosen. For comparison purpose, the results obtained by using our approach are listed in Table I with those from Pentland's variance method and Lundahl et al.'s MLE. From Table I we note that our method will offer estimates of H with less variance, while the bias will be larger than that obtained by the other methods. Roughly speaking, for a fixed data length, the proposed estimator will reduce the variance of the estimates at the expense of increasing their bias.

V. Application to Texture analysis

To illustrate the effectiveness of our method, we now analyze several textured images from the photographic album of Brodatz [11]. These image patterns are discretized to 200×200 pixels with gray level from 0 to 255. The fractal

dimension of 200 horizontal and vertical paths, 51 paths along the 135 and 45 degrees are estimated and denoted by $\hat{D}_h$, $\hat{D}_v$, $\hat{D}_1$, and $\hat{D}_2$, respectively. In Table II, we list the mean and standard deviation of these fractal dimension estimates for each direction of four textured images. We also note that the estimated fractal dimension may be less than 1 along some direction for some texture. This means that the paths cannot be modeled by DFBM and the spectra of the increments of the paths will be steeper than those of DFGN. However, we can still distinguish different textures by the estimated fractal dimension even they are outside the interval (1,2). From Table II, each textured image will be associated with an eight-dimensional feature vector which can be used as an indicator of the roughness of the texture surface. Segmentation by using the feature vector and K-means clustering algorithm can then be applied.

VI. Conclusions

The spectral properties of DFGN have been investigated by numerical computation in this paper. We have found the functional relationship between the PSD of DFGN and the parameter H or fractal dimension. This new D–estimator appears to have a larger bias and smaller variance than those of [3] and [4] in the simulation results. However, we have used the system identification techniques to accomplish the estimation of fractal dimension. This approach will estimate fractal dimension through closed form solutions while [3] is not. Moreover, much computational time has been saved than [4]. In the applications of FBM, for example, the analysis of image textures, can be viewed as a 2D random field. Hence, extension of the model–based approach introduced in this paper to the 2D case will certainly be a direction for future researches.

References

[1] B. B. Mandelbrot, *The Fractal Geometry of Nature*, W. H. Freeman and Company, New York.

[2] B. B. Mandelbrot and J. W. Van Ness, "Fractional Brownian Motions, Fractional Noises and Applications," *SIAM Rev.*, vol. 10, no. 4, pp. 422–437, Oct. 1968.

[3] A. P. Pentland, "Fractal–Based Description of Natural Scenes," *IEEE Trans. Pattern Analysis and Machine Intelligence*, vol. PAMI–6, No. 6, pp. 661–674, Nov. 1984.

[4] T. Lundahl, W. J. Ohley, S. M. Kay, and R. Siffert, "Fractional Brownian Motion: A Maximum Likelihood Estimator and Its Application to Image Texture," *IEEE Trans. Medical Imaging*, vol. MI–5, no 3, pp. 152–161, Sep. 1986.

[5] S. M. Kay, *Modern Spectral Estimation: Theory & Application*, Prentice–Hall, Englewood Cliffs, N.J., 1988.

[6] H. Akaike, "A New Look at the Statistical Model Identification," *IEEE Trans. Autom. Control*, vol. AC19, pp. 716–723, Dec. 1974.

[7] H. B. Mann and A. Wald, "On the Statistical Treatment of Linear Stochastic Difference Equations," *Econometrica*, vol. 11, No. 3 & 4, pp. 173–220, July–Oct. 1943.

[8] H. Akaike, "Power Spectrum Estimation through Autoregressive Model Fitting," *Ann. Inst. Statist. Math.*, vol. 21, pp. 407–419, 1969.

[9] K. N. Berk, "Consistent Autoregressive Spectral Estimates," *Ann. Statist.*, vol. 2, pp. 489–502, 1974.

[10] S. C. Liu, *Model-based Estimation for Fractal Dimension of Fractional Brownian Motion*, Master thesis, National Tsing Hua University, Hsinchu, Taiwan, R. O. C.

[11] P. Brodatz, *Textures: A photographic Album for Artists and Designers*, New York:Dover, 1966.

(a) Our results.

True H	mean($\hat{H}$)	bias($\hat{H}$)	var($\hat{H}$)
0.2	0.2534	0.0534	0.0014
0.4	0.4141	0.0141	0.0005
0.6	0.5831	–0.0169	0.0007
0.8	0.8108	0.0108	0.0014

(b) Results from MLE approach.

True H	mean($\hat{H}$)	bias($\hat{H}$)	var($\hat{H}$)
0.2	0.200	0.000	0.0025
0.4	0.399	–0.001	0.0036
0.6	0.599	–0.001	0.0036
0.8	0.796	–0.004	0.0036

(c) Results from variance approach.

True H	mean($\hat{H}$)	bias($\hat{H}$)	var($\hat{H}$)
0.2	0.196	–0.004	0.0036
0.4	0.392	–0.008	0.0064
0.6	0.591	–0.009	0.0081
0.8	0.778	–0.022	0.0100

Table I. Comparison among the results from (a)our, (b)MLE's, (c)variance's approaches, respectively.

	$\hat{D}_h$		$\hat{D}_v$		$\hat{D}_1$		$\hat{D}_2$	
	mean	std	mean	std	mean	std	mean	std
cork	1.0175	0.0679	1.4084	0.0640	1.7013	0.0512	1.4806	0.0435
stone	0.8618	0.0686	1.3494	0.0742	1.5213	0.0626	1.4339	0.0577
cotton	1.3606	0.0477	1.5867	0.0434	1.6641	0.0281	1.9368	0.0319
bark	0.7277	0.0762	1.1781	0.0748	1.2588	0.0593	1.2968	0.0569

Table II. The mean and standard deviation of estimated fractal dimension along specified directions for textured images.